Laser frequency stabilization based on Sagnac interferometric spectroscopy

Hui Yan (颜 辉)[1,2,3], Guoqing Yang (杨国卿)[1,2,3], Jin Wang (王 谨)[1,2], and Mingsheng Zhan (詹明生)[1,2]

[1]*State Key Laboratory of Magnetic Resonance and Atomic and Molecular Physics, Wuhan Institute of Physics and Mathematics, Chinese Academy of Sciences, Wuhan 430071*

[2]*Center for Cold Atom Physics, Chinese Academy of Sciences, Wuhan 430071*

[3]*Graduate University of Chinese Academy of Sciences, Beijing 100049*

Received July 16, 2007

A simple method based on Sagnac interferometric spectroscopy (SIS) is applied for frequency stabilization of diode lasers. Sagnac interferometric spectra of rubidium vapor are investigated both theoretically and experimentally. The interference signal at the output of the Sagnac interferometer displays a sharp dispersion feature near the atomic resonance. This dispersion curve is used as the feedback error signal to stabilize the laser frequency. Linewidth of a diode laser is stabilized down to 1 MHz by this modulation-free method.

OCIS codes: 300.3700, 300.0300, 140.0140.

Sagnac interferometric spectroscopy (SIS), polarization spectroscopy (PS)[1], and saturation absorption spectroscopy (SAS)[2] are useful Doppler-free spectroscopy methods that in particular can be used for laser frequency stabilization[3−5]. Among them, SAS is more commonly used for laser frequency stabilization due to its narrow spectrum. However, SAS requires frequency modulation and signal lock-in amplification, which prevents it from being adopted in some compact systems. While PS is a modulation-free method for laser frequency stabilization, it is not immune from power fluctuations that could hardly be eliminated in diode lasers. The SIS method can overcome the disadvantages of SAS and PS. Compared against the traditional SAS frequency stabilization method, the SIS method is modulation free and magnetic field free. In addition, in comparative terms the SIS technique is simple and cheap, since it does not depend on costly optoelectronics, function generators, acousto-optical modulators, electro-optical modulators or lock-in amplifier. Furthermore, the SIS method is immune from environment fluctuations and laser power fluctuations. Robins *et al.*[5] initially applied this SIS method to narrow the linewidth of lasers. Since their work was focused on demonstration of the experimental viability of this method, there was no detail qualitative analysis and optimization of the SIS. Thus, it is necessary to investigate this new frequency stabilization method both theoretically and experimentally.

In this letter, we report a theoretical analysis and the experimental results of SIS applied to rubidium vapor. We also study the dependence of the SIS spectrum on the experimental conditions. By using the SIS spectrum as the feedback error signal, we stabilize a diode laser on an atomic resonance, and then optimize the conditions to reach optimal laser frequency stabilization.

The basic operating principle of the SIS includes setting an atom vapor cell into a Sagnac interferometer loop, and then obtaining the atom absorption spectrum. The experimental setup is shown in Fig. 1. As shown in Fig. 1(b), the Sagnac interferometer loop includes three mirrors (M_1, M_2, and M_3) and one beam splitter (BS_1). A rubidium vapor cell (Rb cell 1) and a neutral density filter (NF) are placed into this loop. The anti-clockwise probe beam is set to pass the filter and the Rb cell successively; the clockwise pump beam follows the reverse trajectory. Though the intensities of these two beams are equal at BS_1, they are different when they pass the Rb cell since the probe beam experiences attenuation from the NF. In the end, the anti-clockwise probe beam and the clockwise pump beam combine via the beam splitter (BS_1), and then form interference patterns. The light fields of these two beams are described as

$$E_j(z,t) = \frac{1}{2}E_0 \mathrm{e}^{i(\omega t - k_j z + i\alpha_j z)}, \tag{1}$$

where $j = 1, 2$; k_1, k_2 are the wave vectors of the probe beam and pump beam, respectively; while α_1, α_2 are the respective absorption coefficients related to the probe and pump beams, respectively. Because the pump beam is deeply saturated, the effects of the atom vapor cell can be ignored. The absorption coefficients and wave vectors of the probe and pump beams can be expressed as

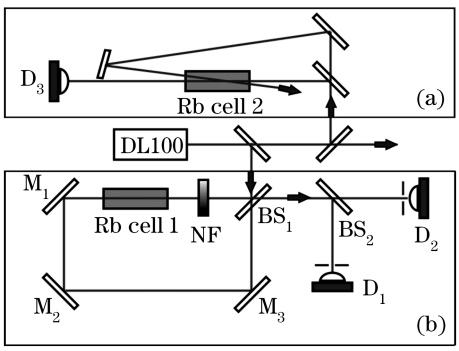

Fig. 1. Diagram of experimental setup. (a) Part for SAS; (b) part for SIS.

$$\alpha_1 = \alpha(\omega), \qquad k_1 = \frac{\omega}{c} n(\omega), \tag{2}$$

$$\alpha_2 = 0, \qquad k_2 = \frac{\omega}{c}. \tag{3}$$

The intensity of the interference signal takes the form of

$$I(\phi) = \frac{1}{4} E_0^2 \mathrm{e}^{-2\alpha(\omega)z} + \frac{1}{4} E_0^2 + \frac{1}{2} E_0^2 \mathrm{e}^{-\alpha(\omega)z} \cos\phi, \tag{4}$$

where

$$\phi = \frac{\omega}{c}[n(\omega) - 1]z \tag{5}$$

and $n(\omega)$ is the refractive index. From Kramers-Kronig dispersion relation, as it has been described in Ref. [6], one can interpret Eq. (4) as a representation of the saturation absorption profile, which is manifested in Fig. 2(a).

One advantage of the SIS is that the dispersion curve can be easily obtained by using tilt locking technique rather than using modulation combined with lock-in amplifying, as it is in conventional spectroscopy method. The principle of tilt locking technique is referred to the use of the spatial mode interference at the output of the Sagnac interferometer. By slightly misaligning the laser beams in the Sagnac loop, the output interference pattern will produce the TEM_{01} mode instead of the TEM_{00} mode, as shown in Fig. 3. Each half of this TEM_{01} mode has a $\frac{\pi}{2}$ phase shift to the TEM_{00} mode, and a π phase shift between themselves[7]. From Eq. (4), we get the intensities of each half of the TEM_{01} mode as

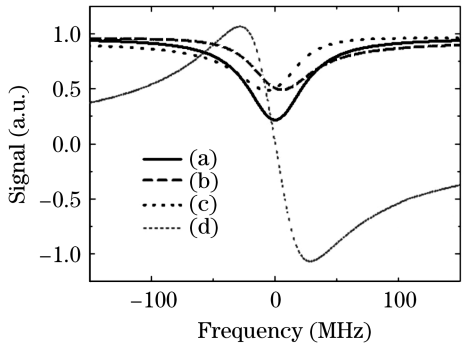

Fig. 2. Qualitative analysis results of the SIS signals. (a) The absorption spectrum of the TEM_{00} mode; (b),(c) the absorption spectra for each half of the TEM_{01} mode; (d) the dispersive curve based on the tilt locking technique.

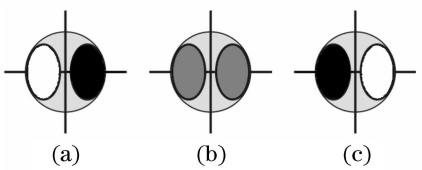

Fig. 3. Spatial distributions of the TEM_{01} mode (panda eyes area) and the TEM_{00} mode (background area). (a)—(c) The spatial distributions of the relative intensity of each half of the TEM_{01} mode when the laser frequency is scanned across an atomic resonance (the white area represents the higher intensity and the black area represents the lower intensity).

$$I_1 = \frac{1}{2} I(\phi - \pi/2), \tag{6}$$

$$I_2 = \frac{1}{2} I(\phi + \pi/2). \tag{7}$$

As it is shown in Fig. 3, the two parts of the TEM_{01} mode are anti-symmetric when the laser frequency is scanned across an atomic resonance. Therefore the intensity difference between these two parts is

$$\Delta I(\phi) = I_1(\phi) - I_2(\phi)$$

$$= \frac{1}{2} E_0^2 \mathrm{e}^{-\alpha(\omega)z} \sin\left\{\frac{\omega}{c}[n(\omega) - 1]z\right\}. \tag{8}$$

According to Kramers-Kronig dispersion relation, it is clear that Eq. (8) is a pure dispersive line shape (Fig. 2(d)). Further more, this line shape is also affected by the whole laser intensity, the length of the Rb cell 1 (z), and the attenuation factor of the NF.

As shown in Fig. 1, the light from the diode laser (DL100) is split into three beams, one beam is for SAS (Fig. 1(a)), one beam is for SIS (Fig. 1(b)), and the other one is for experimental use. We use SAS as a reference signal. The main part is the Sagnac interferometer loop (Fig. 1(b)). In order to obtain the signal for each half of the TEM_{01} mode separately, a beam splitter (BS_2) is used to separate the interference signal, and then the signals are sent to detectors respectively. The difference between these two signals is the right dispersive profile of an atomic resonance, as expressed by Eq. (8).

After adjusting the pump and probe beams to overlap with each other, we tune M_1 or M_2 to the point where the interference signal will change from one spot into two spots, schematically represented in Fig. 3, in order to obtain the TEM_{01} mode as expected. By subtracting the signals from detectors D_1 and D_2, we can get the SIS signal. A careful adjustment of the two detectors will balance the amplitude of the two signals, and also will help to eliminate the effects related to the power fluctuations.

Figure 4 displays the typical experimental signals of the SIS and the SAS. There, P1, P2, and P3 are the absorption peaks of $^{87}\mathrm{Rb}$: $5^2S_{1/2}$, $F = 2 \rightarrow 5^2P_{3/2}$, $F' = 1, 2, 3$ respectively; Co[1,2] is the crossover between P1 and P2, Co[1,3] is the crossover between P1 and P3, and Co[2,3] is the crossover between P2 and P3. Thus from the signal displayed in Fig. 4, it is clear that the dispersion signal from SIS can be used as the error signal to stabilize the

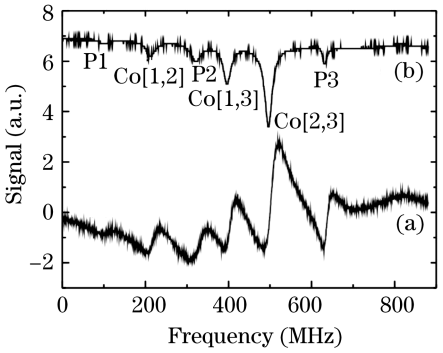

Fig. 4. (a) SIS dispersive signal; (b) the SAS spectrum.

laser frequency. In order to optimize the error signal, we investigated the dependence of error signal on the intensity of probe beam. We found that the best value for the probe laser power is 0.035 mW when the pump laser power is set at 0.35 mW. Namely, the best attenuation factor for the NF is 0.1, as can be seen from the larger peak in the curves shown in Fig. 5.

Thus by selecting the best probe beam power, the error signal can be optimized. Then we lock the frequency of the diode laser (DL100) at the crossover Co[2,3] of ^{87}Rb $F = 2 \rightarrow F' = 2, 3$ resonance by responding the error signal (Fig. 6) to the piezoelectric transducer (PZT) inside the laser head. A digital oscilloscope (TDS3000) is used to monitor the error signal. Figure 7 shows the error signal as a function of time; the system is locked at $t = 6$ s. Without the feedback, the peak-to-peak amplitude of the error signal is 50 mV; it decreased to 10 mV when the feedback is working. The error signal is scaled in two steps. Firstly, the constant difference between two absorption peaks is used to decide the width of every peak, as shown in Fig. 4. Then focusing on one peak, as shown in Fig. 6, the peak-to-peak amplitude of the error signal is 0.5 V, and the corresponding width of the absorption peak is 50 MHz. Thus, the scale value of the error signal is 100 MHz/V. Therefore, the free running linewidth of the diode laser (DL100) is about 5 MHz (This value is also fit for the DL100 specifications), so the resulted linewidth is down to 1 MHz when the feedback is working. This linewidth just represents the short-term stability of the laser. In fact, the more important is the improvement of the long-term stability of the laser frequency. Without the feedback, its frequency drift is more than 100 MHz within one hour (DL100 specifications); with the feedback, it is easy to narrow the frequency drift to 1 MHz within one hour.

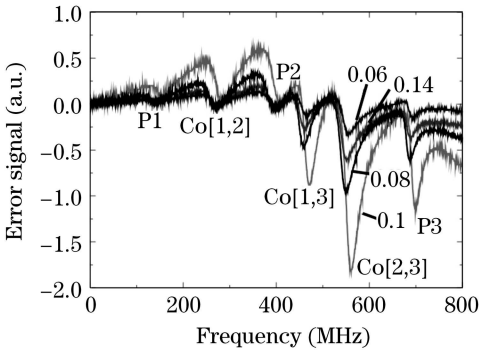

Fig. 5. Experimental SIS dispersive signal of ^{87}Rb at different probe beam powers. The decimal fractions at every line are the ratio of relative intensities between the probe beam and the pump beam. These match with the attenuation factors of the NF.

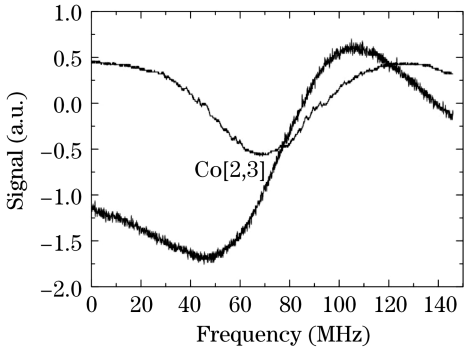

Fig. 6. Proper error signal for feedback to the PZT inside the laser head.

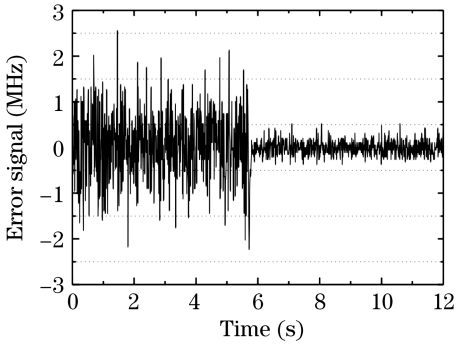

Fig. 7. Amplitude fluctuation of the error signal before and after the feedback.

In conclusion, we have analyzed SIS and its application for laser frequency stabilization. Based on the SIS technique, we built a small system for laser frequency stabilization, and managed to lock the frequency of a diode laser to an atom resonance; the linewidth of the laser was reduced from over 5 MHz down to 1 MHz. The whole system is very compact. It is easy to be miniaturized and integrated in near future.

This work was supported by the National Basic Research Program of China under Grant No. 2005CB724505/1. J. Wang is the author to whom the correspondence should be addressed, his e-mail addressed is wangjin@wipm.ac.cn.

References

1. C. Wieman and T. W. Hansch, Phys. Rev. Lett. **36,** 1170 (1976).
2. V. S. Letokov and V. P. Chebotayev, *Nonlinear Laser Spectroscopy* (Springer-Verlag, Berlin, 1977).
3. K. B. MacAdam, A. Steinbach, and C. Wieman, Am. J. Phys. **60,** 1098 (1992).
4. K. Jiang, J. Wang, X. Tu, M. He, and M. Zhan, Chin. Opt. Lett. **1,** 377 (2003).
5. N. P. Robins, B. J. J. Slagmolen, D. A. Shaddock, J. D. Close, and M. B. Gray, Opt. Lett. **27,** 1905 (2002).
6. W. Demtröder, *Laser Spectroscopy — Basic Concepts and Instrumentation* (Springer-Verlag, Berlin, 1996) p.459.
7. D. A. Shaddock, M. B. Gray, and D. E. McClelland, Opt. Lett. **24,** 1499 (1999).